

Analysis of Muscle Synergy Contribution on Human Standing-up Motion Using a Neuro-Musculoskeletal Model

Qi An¹, Yuki Ishikawa¹, Shinya Aoi², Tetsuro Funato³, Hiroyuki Oka⁴,
Hiroshi Yamakawa¹, Atsushi Yamashita¹, and Hajime Asama¹

Abstract—It is important to understand the mechanism of human standing-up motion to improve the declined physical ability of the elderly people. This study employs the concept of muscle synergies (modular structure of coordinative muscle activation) to understand how humans coordinate their muscles to achieve the standing-up motion. Neuro-musculoskeletal model was developed to represent human body to generate standing-up motion. Using the developed model, forward dynamic simulation was used to analyze how humans utilized the muscle synergies to realize the motion. Results showed that the developed model could generate the standing-up motion with four muscle synergies rather than controlling individual muscles. Moreover, further analysis showed that three different strategies of the standing-up motion could be generated only by changing the start time of the particular muscle synergy.

I. INTRODUCTION

The aging society has brought serious healthcare issues; such as increased social security cost, mental and physical stress to caregivers, and declined physical ability. In order to improve the situation and quality of life of the elderly, standing-up motion is focused. Human standing-up motion is an important which many daily activities follow after that.

In robotic research, many devices have been developed to assist the standing-up motion. For example, our research group previously developed the assistive system which was composed of a bed and a bar to lead human body to the desired trajectory [1]. Another device is a chair type to utilize the gravitational force to lift up the hip of the users to achieve the standing-up motion [2]. Different from these devices, robotic exoskeleton devices have been also proposed to detect human intention of standing-up motion and to generate compensative torque on their joints [3].

In order to fully utilize these devices, it is important to understand the mechanism of how humans realize the standing-up motion. Considering human behavior, their body is redundant system that there are more muscles to be controlled than the number of joints. In order to clarify how humans coordinate their redundant numbers of muscles, the concept of muscle synergy is employed. Muscle synergy has been firstly proposed by Bernstein [4] to suggest that humans

¹Qi An, Yuki Ishikawa, Hiroshi Yamakawa, Atsushi Yamashita, and Hajime Asama: the Department of Precision Engineering, Graduate School of Engineering, The University of Tokyo, Tokyo, Japan anqi@robot.t.u-tokyo.ac.jp

²Shinya Aoi: the Department of Aeronautics and Astronautics, Graduate School of Engineering, Kyoto University, Kyoto, Japan

³Tetsuro Funato: the Department of Mechanical Engineering and Intelligent Systems, The University of Electro-Communications, Tokyo, Japan

⁴Hiroyuki Oka: the 22nd Century Medical and Research Center, Graduate School of Medicine, The University of Tokyo, Tokyo, Japan

movement could be generated from the limited number of modules (called synergy) although human movements were varied. In the previous studies regarding the muscle synergies [5][6], they collected data of human behaviour and to show that variant human movements could be explained by the small number of muscle synergies. However, these studies could not clarify how each synergy contributed to the success of the motion since they especially focus on the controlled and succeed trials. In fact, it is difficult to observe failed human motion due to ethical and safety issues. In order to overcome this problem, we develop the human neuro-musculoskeletal model and employ the simulation methodology to understand how the muscle synergy affects the movement. If the model could emulate human behavior, it would be useful to understand the mechanism of the motion. Therefore the objective is firstly to show that the developed model could generate the standing-up motion similar to humans. Next, we show that human standing-up motion is changed according to the muscle synergy.

II. NEURO-MUSCULOSKELETAL SYSTEM

Figure 1 shows a schematic diagram of the developed neuro-musculoskeletal model. It is composed of three components: nervous system, skeletal model, and muscle model. Nervous system has two components: muscle synergy and postural control. Muscle synergy generates muscle activation \mathbf{M} and postural control generates joint torque \mathbf{T}_{fb} to stabilize the body posture. When muscle model receives muscle activation \mathbf{M} , it calculates joint torque \mathbf{T}_{mus} . Dynamics of muscle property is also taken into account by considering body posture Θ and $\dot{\Theta}$. Joint torque \mathbf{T}_{jnt} is calculated from summation of \mathbf{T}_{mus} and \mathbf{T}_{fb} . Skeletal model calculates body kinematics when it receives joint torque \mathbf{T}_{jnt} . Detailed description of each component is explained below.

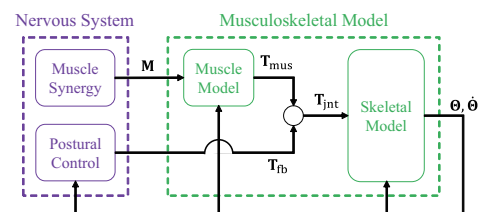


Fig. 1. Developed Neuro-musculoskeletal System. Nervous system generates muscle activation \mathbf{M} and postural stabilizing torque \mathbf{T}_{fb} . Muscle model generates joint torque \mathbf{T}_{mus} from muscle activation and dynamics of muscle property considering body posture. Skeletal model calculates body kinematics Θ and $\dot{\Theta}$ from joint torque \mathbf{T}_{mus} and \mathbf{T}_{fb} .

A. Skeletal Model

This study divided human body into four segments such as thigh, shank, pelvis, and HAT (head, arm and trunk) as in Fig. 2 (a). Joint angle $\theta_{k=1,2,3,4}$ respectively indicates the angle from the distant segment for ankle, knee, hip, and trunk joints. Skeletal model calculates body kinematics from the following equation of motion.

$$\mathbf{I}(\Theta)\ddot{\Theta} + \mathbf{h}(\Theta, \dot{\Theta}) + \mathbf{g}(\Theta) + \mathbf{D}(\Theta, \dot{\Theta}) = \mathbf{T}_{\text{jnt}} + \Phi(\Theta, \dot{\Theta}), \quad (1)$$

where $\mathbf{I}(\Theta)$, $\mathbf{h}(\Theta, \dot{\Theta})$, and $\mathbf{g}(\Theta)$ indicate matrices of inertia, non-linear force, and gravitation terms respectively. $\mathbf{D}(\Theta, \dot{\Theta})$ has an element d_k to represent resistant force exerted on each joint as in eq. (2). According to the anatomical knowledge, each joint receives resistant force based on joint angles for the ankle, knee, and hip joints and angular velocities for the trunk when humans move their joints [7][8].

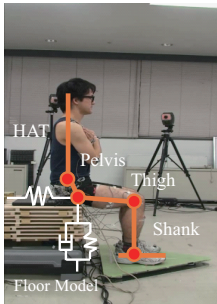
$$\mathbf{D}(\Theta, \dot{\Theta}) = \begin{cases} d_k \dot{\theta}_k & \text{when } k = 1, 2, 3 \\ d_k^{\text{ext}} \theta_k & \text{when } k = 4, \theta_k > 0.0314 \\ d_k^{\text{flx}} \theta_k & \text{when } k = 4, \theta_k < -0.0314 \end{cases} \quad (2)$$

Additionally, $\Phi(\Theta, \dot{\Theta})$ represents vertical and horizontal reaction force which is applied to the hip joint with kinetic and elastic elements when the hip joint is lower than the chair height H . In the eq. (1), \mathbf{T}_{jnt} indicates joint torque which is generated from muscle model and postural control.

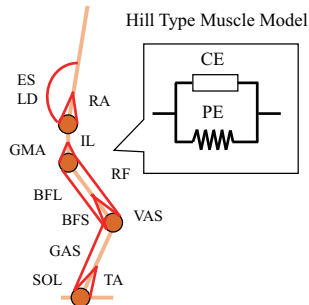
B. Muscle Model

The muscle model generates joint torque \mathbf{T}_{mus} . In this study, 12 muscles were considered including mono- and bi-articular muscles in both upper trunk and lower limbs as in Fig. 2 (b): tibialis anterior (TA), soleus (SOL), gastrocnemius (GAS), rectus femoris (RF), vastus lateralis (VAS), biceps femoris long head (BFL), biceps femoris short head (BFS), gluteus maximus (GMA), iliopsoas (IL), recutus abdominis (RA), elector spine (ES), and latissimus dorsi (LD).

In order to calculate the muscular tension, hill type muscle model is employed [9]. Muscular tension F_i is obtained from two components (eq. (4)): contractile element (CE) generates muscular tension F_i^{CE} actively and parallel element (PE)



(a) Skeletal Model



(b) Muscle Model

Fig. 2. Musculoskeletal Model. (a) Skeletal Model. Human body is divided into four parts: shank, thigh, pelvis and HAT (head and trunk). Kinetic and damping elements are used to express floor model. (b) Muscle Model. Twelve muscles are considered including bi-articular muscles. Hill type muscle model is used to represent muscles.

generates tension F_i^{PE} passively when it is extended. Joint torque of each joint τ_k is calculated from multiplication of moment arm r_{ki} and muscular tension F_i . r_{ki} is the moment arm of muscle i to the joint k . r_{ki} is zero if the muscle i does not attach the joint k , and it is either positive or negative value depending on the contribution of each muscle (flexor or extensor). Force generated from CE in muscle i is calculate from eq. (5). In the equation, F_i^{max} is maximum contraction force and it is determined from anatomical data. Also, muscular dynamic property is considered as muscle force-length relationship (f_{fl}) and force-velocity relationship (f_{fv}) as in eqs. (6–7) [10][11]. In the equations, \tilde{l}_i is normalized muscular length and it is calculated by muscular length l_i divided by optimal length of each muscle l_i^o . Muscle length is determined from moment arm r_{ki} and joint angle θ_k [12]. Also, \tilde{v}_i is normalized muscular contraction velocity which is obtained from muscular velocity divided by ten times of muscle optimal length. Force generated in PE is calculated from eq. (8); it generates muscular force only when it is extended from the optimal length [13].

$$\tau_k = \sum_{i=1}^4 \sum_{j=1}^{12} r_{ki} F_i, \quad (3)$$

$$F_i = F_i^{\text{CE}} + F_i^{\text{PE}}, \quad (4)$$

$$F_i^{\text{CE}} = F_i^{\text{max}} f_{\text{fl}} f_{\text{fv}} m_i, \quad (5)$$

$$f_{\text{fl}} = \exp(-(\tilde{l}_i - 1)^2), \quad (6)$$

$$f_{\text{fv}} = 1 + \tanh(\tilde{v}_i), \quad (7)$$

$$F_i^{\text{PE}} = \begin{cases} 0 & \tilde{l}_i < 1.0 \\ F_i^{\text{max}} \frac{e^{10(\tilde{l}_i - 1)}}{e^5} & 1.0 \leq \tilde{l}_i \leq 1.5 \\ F_i^{\text{max}} & 1.5 < \tilde{l}_i \end{cases} \quad (8)$$

C. Nervous System

1) *Muscle Synergy Model*: In this study, muscle activation is expressed as a linear summation of spatial and temporal patterns of muscle synergies as in eq. (9).

$$\mathbf{M} = \mathbf{W}\mathbf{C}, \quad (9)$$

$$\mathbf{M} = \begin{pmatrix} \mathbf{m}_1(t) \\ \mathbf{m}_2(t) \\ \vdots \\ \mathbf{m}_n(t) \end{pmatrix} = \begin{pmatrix} m_1(1) & \cdots & m_1(T_{\text{max}}) \\ \vdots & \ddots & \vdots \\ m_n(1) & \cdots & m_n(T_{\text{max}}) \end{pmatrix}, \quad (10)$$

$$\mathbf{W} = (\mathbf{w}_1 \cdots \mathbf{w}_N) = \begin{pmatrix} w_{11} & \cdots & w_{1N} \\ \vdots & \ddots & \vdots \\ w_{n1} & \cdots & w_{nN} \end{pmatrix}, \quad (11)$$

$$\mathbf{C} = \begin{pmatrix} \mathbf{c}_1(t) \\ \mathbf{c}_2(t) \\ \vdots \\ \mathbf{c}_N(t) \end{pmatrix} = \begin{pmatrix} c_1(1) & \cdots & c_1(T_{\text{max}}) \\ \vdots & \ddots & \vdots \\ c_N(1) & \cdots & c_N(T_{\text{max}}) \end{pmatrix}. \quad (12)$$

In eq. (10), \mathbf{M} is muscle activation matrix in which each row $\mathbf{m}_{j=1,2,\dots,N}$ expresses excitation level of n different muscles at time t ($1 \leq t \leq T_{\text{max}}$). Matrices \mathbf{W} and \mathbf{C} show spatial and temporal patterns of muscle synergy model. Spatial pattern \mathbf{W} defines relative excitation level of muscles in muscle synergies. Its column \mathbf{w}_j shows the vector to represent N different spatial patterns (eq. (11)). On the other hand, matrix \mathbf{C} indicates temporal patterns of muscle synergy model (eq. (12)). Each row shows time-varying weighting coefficient \mathbf{c}_j to scale the amplitude of spatial pattern \mathbf{w}_j .

Figure 3 shows a schematic design of muscle synergy model. It assumes that n muscle activation is generated from three muscle synergies. Figure 5 (a) illustrates spatial patterns of muscle synergies ($\mathbf{w}_{1,2,3}$) and it determines fixed excitation level of muscles. On the other hand, the corresponded temporal patterns $\mathbf{c}_{1,2,3}$ define a time-varying scaling coefficient of each synergy (Fig. 3 (b)). In Fig. 5 (c), blue, red, and green dashed lines respectively show muscle activation which is generated from each muscle synergy. Gray area shows the summation of these activation $\mathbf{m}_{1,2,3,\dots,n}$.

2) *Postural Control*: Postural control stabilize the posture of the skeletal model. In this study, PD control is used to calculate the postural stabilization torque as in eqs. (13–14). In the equation, $\Delta\mathbf{q}$ and $\Delta\dot{\mathbf{q}}$ indicate difference between reference joint angle (angular velocity) and that of the skeletal model. Reference joint angle is calculated from the horizontal direction. \mathbf{K}_P^q , \mathbf{K}_D^q , and $\mathbf{K}_D^{\dot{q}}$ are coefficients for PD control. The nervous transmission delay time is also taken into account as λ . In order to limit the effect of postural control on body kinematics, the range of joint torque is set to be between τ_{fb}^{\min} and τ_{fb}^{\max} .

$$\mathbf{T}_{fb} = \mathbf{K}_P^q \Delta\mathbf{q}(t) + \mathbf{K}_D^q d\Delta\mathbf{q}(t) + \mathbf{K}_D^{\dot{q}} d\Delta\dot{\mathbf{q}}(t), \quad (13)$$

$$\Delta\mathbf{x}(t) = \hat{\mathbf{x}}(t - \lambda) - \mathbf{x}(t - \lambda). \quad (14)$$

III. FORWARD DYNAMIC SIMULATION

In this study, forward dynamic simulation is conducted to calculate how body kinematics is generated from the developed muscle synergy model. Firstly, spatiotemporal patterns of muscle synergy need to be decided. To begin with, inverse dynamics is used to obtain joint torques during the standing-up motion. Next, muscle activation is determined in order to successfully generate the necessary muscular tension for the standing-up motion. However, muscle activation cannot be calculated exclusively since some muscles are bi-articular muscles (GAS, RF, and BFL) and one of the muscles (IL) cannot be measured due to the inner muscle. In this study, optimization methodology is used to calculate muscle activation \mathbf{m}_i to minimize the following squared error z in eq. (15) under the constraints which muscle activation \mathbf{m}_i can generate the necessary joint torques to achieve

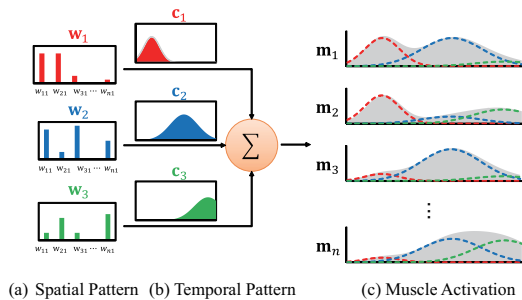


Fig. 3. Muscle Synergy Model. (a) shows spatial patterns ($\mathbf{w}_{1,2,3}$) which indicates relative excitation level of each muscle. (b) shows temporal patterns ($\mathbf{c}_{1,2,3}$) to define time-varying weighting coefficient of corresponded muscle synergies. (c) shows time-varying activation for n muscles (gray part). Red, blue, and green dashed lines show generated activation from muscle synergies 1, 2, and 3 respectively.

the motion. In the equation, \mathbf{m}'_i is the muscle activation measured from a human subject.

$$z = \sum_{i=1}^n \frac{1}{2} \|\mathbf{m}_i - \mathbf{m}'_i\|^2. \quad (15)$$

Spatiotemporal patterns of muscle synergies are calculated from muscle activation \mathbf{m} using non-negative matrix factorization algorithm [14]. In order to decide the number of muscle synergies, one-factor analysis of variance (ANOVA) is employed to evaluate the effect of the number of muscle synergies on the performance to represent observed muscle activation. When there is a statistical significance, a post-hoc test was applied to the neighbouring number of synergies. In this study, temporal patterns of muscle synergies are expressed as a trapezoid wave in order to avoid the effect of artifact and noise of surface electromyography.

Forward dynamic simulation is used for calculating body kinematics. Firstly, initial posture is given to the developed model. Next, temporal pattern $\mathbf{c}_j(t)$ is input to the muscle synergy model to generate muscle activation $\mathbf{m}(t)$ by multiplication of spatial pattern \mathbf{w}_j . When the muscle model receives muscle activation $\mathbf{m}(t)$, it generates joint torque \mathbf{T}_{jnt} . At last, the skeletal model calculates body kinematics Θ and $\dot{\Theta}$ from joint torque \mathbf{T}_{jnt} and postural stabilizing torque \mathbf{T}_{fb} . For numerical calculation, fourth order Runge-Kutta method is employed with time interval 1 ms, and it is calculated using MATLAB.

A. Effect of Muscle Synergy Start Time

From the previous study [5], it is known that temporal patterns of muscle synergy were varied in their amplitude and peak time. In this study, we especially focus on how the start times of the muscle synergy affects the standing-up motion. Using the developed neuro-musculoskeletal model, it is evaluated how individual muscle synergy contribute to the achievement of the standing-up motion. In this study, especially start time of the muscle synergy is focused.

$$\mathbf{m}(t) = \sum_{j=1}^N \mathbf{w}_j \mathbf{c}_j(t - \delta_j). \quad (16)$$

In order to assess how the different start time of muscle synergies affect the human standing-up motion, the horizontal and vertical center of mass (CoM) positions were evaluated. If there is a CoM position which vertical position is above the height threshold η and horizontal position is on the feet support area, it is considered as the model realizes the standing-up motion. Otherwise, it is assessed as the model can not generate the movement; it results in falling either forward or backward (when the horizontal CoM position is not on the feet), or unable to lift up the body (when the vertical CoM position is below the height threshold η).

B. Empirical Experiment with Human

In this study, measurement experiment was conducted in order to validate the results of the simulation and to decide some of the parameters for the forward dynamic simulation. One healthy young male participated (27 years, 1.77 m, 80 kg) at our experiment. During the experiment, body

kinematics was measured in 200 Hz by optical motion capture system with eight cameras (MAC3D; Motion Analysis Corp.). Floor reaction force was measured in 64 Hz from the hip and the feet with two forceplates. Muscle activation was recorded in 1,000 Hz with the surface electromyography sensors (DL-141; S&ME Corp.).

The chair height was set to the knee height of the subject. At the beginning of the experiment, the subject was asked to have their arm crossed in front of their chest. Also, his shank was put vertically to the ground. Motion speed of the standing-up was not controlled clearly, and the subject was asked to stand up in the comfortable speed. In total, 17 trials of the standing-up motion were recorded, and all the trials of the motion were normalized according to the time of hip rising. 1.0 s before and 1.0 s after the time was used. All the data is filtered with second order butter worth low-pass filter in 10, 25, and 25 Hz respectively for body kinematics, reaction force, and muscle activation. This experiment was conducted with approval by the Institute Review Board (IRB) of The University of Tokyo.

IV. RESULTS

A. Muscle Synergy

Figure 4 shows how the coefficient of determination changed according to the number of muscle synergies. It shows that statistical significance increased until four muscle synergies, and adding more synergies did not increase the performance of synergies. In addition, it shows that four muscle synergies could account for more than 95% of measured muscle activation which was the criterion threshold of the previous study [15]. Therefore, in this study, the number of muscle synergies was decided as four.

Figure 5 shows spatiotemporal patterns of muscle synergies which are used for the forward dynamic simulation. Figure 5 (a) shows spatial patterns of muscle synergies. Blue, red, green, and black bars respectively show relative excitation level of muscles including in muscle synergies 1, 2, 3, and 4. Each synergy had particular contribution toward body kinematics according to the anatomical knowledge. Muscle synergy 1 mostly activated RA which flexed the upper trunk to generate momentum necessary for the standing-up motion. Muscle synergy 2 activated TA which dorsiflexed ankle joint to move the center of mass (CoM) forward. Muscle synergy 3 mainly activated VAS (knee extensor)

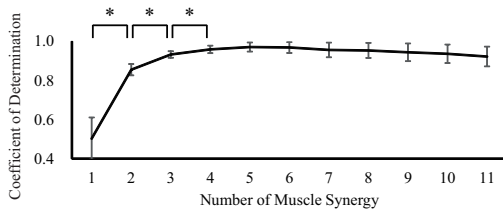


Fig. 4. Coefficient of Determination. Above figure shows how the coefficient of determination is changed according to the number of muscle synergies. It shows that statistical significance increased until four muscle synergies. Additionally it shows that four muscle synergies could account for more than 95% of muscle activation.

and ES (trunk extensor) to extend the whole body to move the CoM upward. Muscle synergy 4 activated SOL (ankle plantarflexion) to decelerate CoM movement.

B. Generated Movement

Kinetic and elastic coefficients were set to be 10,000 kg/s² and 300 kg/s for the vertical direction, and elastic coefficient was set to be 400 kg/s for the horizontal direction. Chair height H was set to be 0.555 m. Proportional and derivative gains for PD control were set as follows: $\mathbf{K}_P^q = [250, 350, 80, 400]$, $\mathbf{K}_D^q = [33500, 43500, 1570, 41000]$, and $\mathbf{K}_D^{\dot{q}} = [1500, 1000, 70, 2500]$. The same parameters of body segment and muscles are used as the previous study [16]. Nervous transmission delay time λ was set to be 100 ms. Maximum and minimum joint torques to stabilize posture (τ_{fb}^{\min} and τ_{fb}^{\max}) were set to be -50 and 50 Nm.

Figure 6 shows generated torques from muscle synergy (\mathbf{T}_{jnt} : solid lines) and postural control (\mathbf{T}_{fb} : dashed lines): (a) ankle, (b) knee, (c) hip, and (d) trunk. These results show that the joint torques were mainly generated from four muscle synergies rather than postural control.

Figure 7 shows generated movement of standing-up motion from the forward dynamic simulation. Figure 7 (a) shows comparison of joint angles between measured (dashed lines) and simulated angles (solid lines): red, blue, green, and black lines respectively indicate ankle, knee, hip, and trunk joints. Figures 7 (b-c) show comparison of floor reaction force between simulation (solid line) and measurement (dashed line) for hip and foot joints: blue and red lines show floor reaction force in the vertical and horizontal directions. Although the foot joint is fixed in the proposed model, foot reaction force was calculated using a method of Lagrange multiplier. Our simulation results showed that four muscle synergies could successfully generate human standing-up motion.

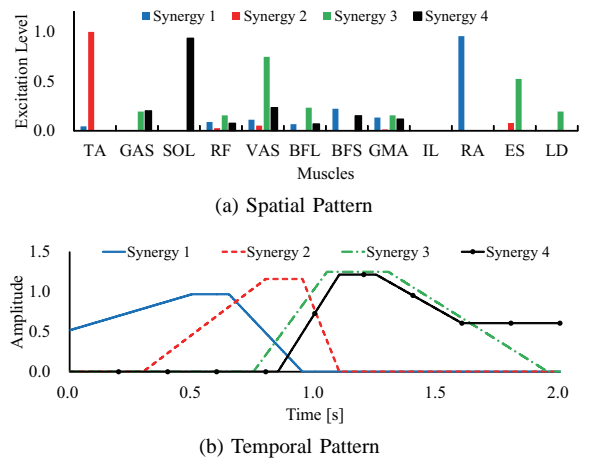


Fig. 5. Spatiotemporal Pattern of Muscle Synergy. (a) Spatial Pattern. Above bars show relative excitation level of muscles. Each synergy has characteristic muscle activation. (b) Temporal Pattern. Each muscle synergy is activated in clear order from muscle synergies 1 to 4.

C. Different Strategy of Standing-up Motion

In this study, the effect of the muscle synergy 3 was especially focused. Spatial patterns of the muscle synergy 3 showed that it mainly extended the knee and trunk joints to move CoM upward. Therefore the muscle synergy 3 is regarded as important to change the posture from sitting to standing. Using the developed model, it is evaluated how the standing-up motion is affected by the muscle synergy 3. Figure 8 shows how body kinematics were changed. X and y axes respectively show time series of horizontal and vertical CoM positions. Feet support area was shown in gray area of the graph and it was decided from -0.1 m to 0.2 m when

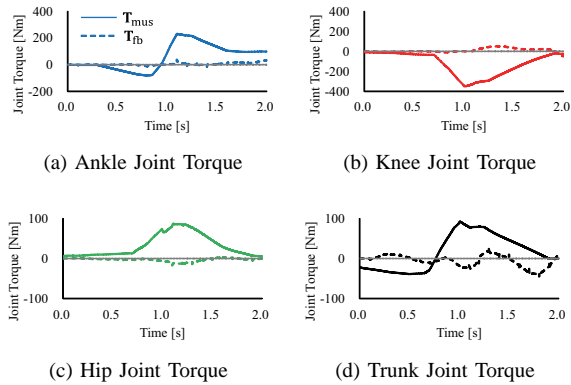


Fig. 6. Generated Joint Torque from Muscle Synergy and Postural Control. (a)–(d) show ankle, knee, hip, and trunk joint torques respectively.

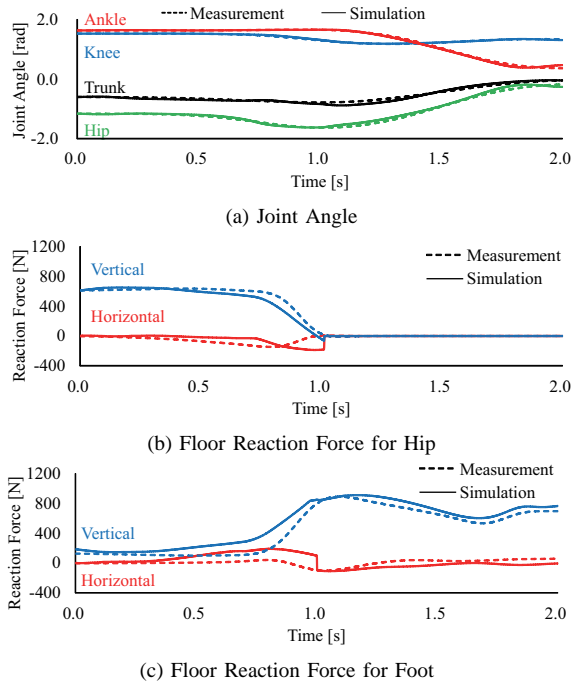


Fig. 7. Generated Standing-up Motion. (a) Joint Angle. It shows comparison between simulated kinematics (solid line) and measured one (dashed line). (b-c) Floor Reaction Force for Hip and Foot. It shows comparison between simulated floor reaction force and measured one for hip and foot.

the ankle position was set to be the origin (0.0 m). Also, the height threshold η was set to be 1.0 m. In the simulation procedure, only the start time of the muscle synergy 3 was changed from -100 ms to 100 ms with an interval of 50 ms and other parameters were remained the same. The models started from left bottom of the graph (described as “Sitting”) to the right top (described as “Standing”). In Fig. 8 (a), the CoM trajectories are shown: green, blue, black, red, and gray lines show trajectories generated respectively from different start times ($\delta_3 = -100, -50, 0, 50, 100$ ms).

When the muscle synergy 3 started earlier (i.e. δ_3 is smaller), the models started moving upward earlier. However, the model could not achieve the standing-up motions when δ_3 was -100 ms because it did not reach the height threshold η . In other cases, the model satisfied the criteria of horizontal and vertical positions. Focusing on the success trials, different characteristic kinematics were generated. The difference was mainly found in the time of upward movement. When the muscle synergy 3 started comparatively earlier ($\delta_3 = -50$ ms), the model moved upward although their horizontal CoM position was below the feet. On the contrary, the model did not lift up their body until the horizontal CoM was on the feet ($\delta_3 = 50$ ms). This implied that humans possibly changed the time of lifting up their body. Figure 8 (b) shows stick pictures of three generated standing-up motion ($\delta_3 = -50, 0, 50$ ms). Around the time 1.0–1.2 s, the model inclined their trunk more when δ_3 was 50 ms. On the other hand, the model already began upward movement before their horizontal CoM was on the feet when δ_3 was -50 ms.

V. DISCUSSION

We have developed the neuro-musculoskeletal model to represent human body based on body dynamics and anatomi-

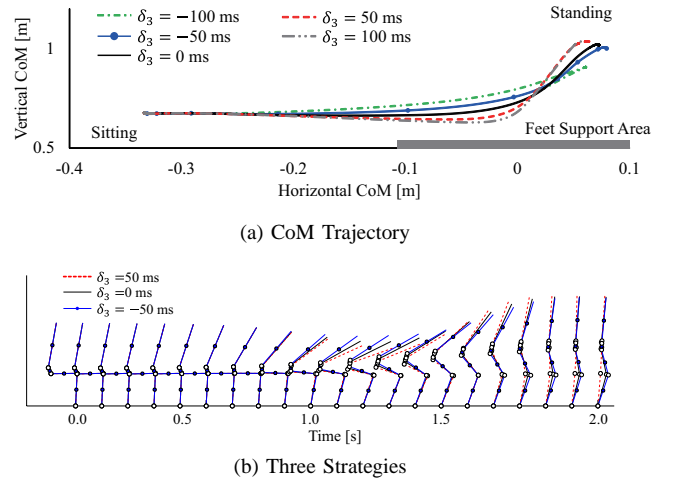


Fig. 8. Three Strategies of Standing-up Motion. (a) It shows CoM trajectory of three standing-up motions. X and y axes show horizontal and vertical positions of CoM. Gray square shows the feet support area. In these examples, start times of muscle synergy 3 (δ_3) were changed from -100 ms to 100 ms with the interval of 50 ms. (b) It illustrates movement of stick pictures performing different strategies of standing-up motion.

cal knowledge. Using the developed model, forward dynamic simulation showed that four muscle synergies could successfully realize the standing-up motion.

Moreover, it was analyzed how the muscle synergy 3 affects the standing-up motion. Results showed that the start time of muscle synergy 3 could control the time of upward CoM movement. When the muscle synergy 3 started earlier, the model began moving upward although its horizontal CoM was below the feet. On the other hand, when the synergy started later, the model lifted up the body after its CoM was on the feet. The same characteristic movements were also reported in the previous study [17]. The literature classified the standing-up motions into three strategies based on the CoM trajectories: momentum transfer, hybrid, and stabilization strategies. In the momentum transfer strategy, they start moving upward earlier than other two strategies. However, in the stabilization strategy, they do not move upward until they move their CoM on feet. CoM trajectory of the hybrid strategy exists in the middle of above two strategies. It was also pointed out that the elderly people tended to use the stabilization strategy. In the stabilization strategy, the moment arm of the body CoM is shorter than that of the momentum transfer strategy. Therefore, the required knee joint torque became less in the stabilization than the momentum transfer strategy. The momentum transfer strategy usually utilize the generated momentum to stand up even their horizontal CoM is below the feet support area.

The main function of muscle synergy 3 was to extend the whole body by activation of VAS and ES. Therefore, the momentum transfer strategy is likely chosen when muscle synergy 3 started earlier to move the CoM upward. However, the standing-up motion resulted in failure when the muscle synergy 3 started too early ($\delta_3 = -100$ ms) due to longer moment arm of CoM position and insufficient momentum. On the other hand, muscle synergy 3 started comparatively later in the stabilization strategy to firstly move the CoM closer to their feet by the former two synergies.

One of the contribution of our study will be detection of motion strategy of the standing-up motion. In order to assist the human motion effectively, it is important to clarify what strategies they are employing during the motion. Our finding suggested that standing-up motion strategies could be determined from the start time of muscle synergy 3. Therefore it enables the assistive system to adaptively change their movement patterns based on the real time detection of start time of the muscle synergy 3.

VI. CONCLUSIONS AND FUTURE STUDY

In this study, neuro-musculoskeletal model was developed to represent human body. Using the model, it was validated that four muscle synergies could generate human standing-up motion rather than controlling individual muscles. Moreover, our forward dynamic simulation results showed that three different motion strategies (momentum transfer, hybrid, and stabilization) could be generated by controlling the start time of muscle synergy 3.

Our future study is examination of how other synergies affect the standing-up motion. Specifically, it is needed to clarify how the muscle synergy 1 (trunk flexion) generates necessary momentum for the motion. Also, further improvement of the model is necessary to represent different human situation. For example, if the model is adjusted to the elderly persons, it would be expected to fully understand how they prefer the stabilization strategy than others.

ACKNOWLEDGEMENT

This work was in part supported by JSPS KAKENHI Grant Number 24300198, 26120005, 26120006, JST RISTEX Service Science, Solutions and Foundation Integrated Research Program, and Grant-in-Aid for JSPS Fellows 24-8702.

REFERENCES

- [1] Chugo D, Okada E, Kawabata K, Kaetsu H, Asama H, Miyake N, and Kosuge K, "Force Assistance System for Standing-up Motion". *Industrial Robot: An International Journal*, vol. 34, pp. 128-134, 2007.
- [2] Agrawal SK, Caltim G, Fattah A, and Hamnett J, "Design of a Passive Gravity-Balanced Assistive Device for Sit-to-Stand Tasks", *Journal of Mechanical Design, Transactions of the ASME*, vol. 128, pp. 1122-1129, 2006.
- [3] Kawanishi R, Hasegawa Y, Tsukahara A, and Sankai Y, "Sit-to-Stand and Stand-to-Sit Transfer Support for Complete Paraplegic Patients with Robot Suit HAL" *Advanced Robotics*, vol. 24, pp. 1615-1638, 2010.
- [4] Bernstein N, "The Co-ordination and Regulation of Movement". Pergamon, Oxford, 1967.
- [5] Yuri P, Ivanenko YP, Cappellini G, Dominici N, Poppele RE and Lacquaniti F, "Five Basic Muscle Activation Patterns Account for Muscle Activity during Human Locomotion", *Journal of Physiology*, vol. 556, pp. 267-282, 2004.
- [6] Weiss EJ and Flanders M, "Muscular and Postural Synergies of the Human Hand". *Journal of Neurophysiology*, vol. 92, pp. 5235-535, 2004.
- [7] Davy DT and Audu ML, "A Dynamic Optimization Technique for Predicting Muscle Forces in the Swing Phase of Gait", *Journal of Biomechanics*, vol. 20, pp. 187-201, 1987.
- [8] Christophy M, Faruk Senan NA, Lotz JC, and O'Reilly OM, "A Musculoskeletal Model for the Lumbar Spine", *Biomechanics and Modeling in Mechanobiology*, vol. 11, pp. 19-34, 2012.
- [9] Zajac FE, "Muscle and Tendon: Properties, Models, Scaling, and Application to Biomechanics and Motor Control", *Critical Reviews in Biomedical Engineering*, vol. 17, pp. 359-411, 1989.
- [10] Ogihara N and Yamazaki N, "Generation of Human Bipedal Locomotion by a Bio-mimetic Neuro-musculo-skeletal Model", *Biological Cybernetics*, vol. 84, pp. 1-11, 2001.
- [11] Hatze H, "Myocybernetic Control Models of Skeletal Muscles", *Biological Cybernetics*, vol. 25, pp. 103-119, 1977.
- [12] Riener R and Fuhr T, "Patient-Driven Control of FES-supported Standing up: A Simulation Study", *IEEE Transactions on Rehabilitation Engineering*, vol. 6, pp. 113-124, 1998.
- [13] Kuo P and Deshpande AD, "Contribution of Passive Properties of Muscle-tendon Units to the Metacarpophalangeal Joint Torque of the Index Finger", *Proceedings of the 2010 IEEE RAS&EMBS International Conference on Biomedical Robotics and Biomechanics (BioRob2010)*, pp. 288-294, 2010.
- [14] Lee DD and Seun HS, "Learning the Parts of Objects by Non-negative Matrix Factorization", *Nature*, vol. 401, pp. 788-791, 1999.
- [15] Ting LH and Macpherson JM, "A Limited Set of Muscle Synergies for Force Control During a Postural Task", *Journal of Neurophysiology*, vol. 93, pp. 609-613, 2005.
- [16] An Q, Ishikawa Y, Aoi S, Funato T, Oka H, Yamakawa H, Yamashita A, Asama H, "Muscle Synergy Analysis of Human Standing-up Motion Using Forward Dynamic Simulation with Four Body Segment Model", *Proceedings of the International Symposium on Distributed Autonomous Robotic System (DARS2014)*, 2014 (In Press).
- [17] Hughes MA, Weiner DK, Schenkman ML, Long RM, and Studenski SA, "Chair Rise Strategies in the Elderly". *Clinical Biomechanics*, vol. 9, pp. 187-192, 1994.